



ELSEVIER

Earth and Planetary Science Letters 6022 (2001) 1–15

EPSL

www.elsevier.com/locate/epsl

Estimate of inner core rotation rate from United Kingdom regional seismic network data and consequences for inner core dynamical behaviour

Jonathan D. Collier^{a,*}, George Helffrich^{a,b}^a Department of Earth Sciences, University of Bristol, Wills Memorial Building, Queen's Road, Bristol BS8 1RJ, UK^b Earth and Planetary Sciences Department, Tokyo Institute of Technology, 2-12-1 Ookayama, Meguro-ku, Tokyo 152-8551, Japan

Received 4 June 2001; received in revised form 11 September 2001; accepted 19 September 2001

Abstract

We analyse over 12 500 records of southwest Pacific earthquakes recorded by the UK network for PKP_{BC} and PKP_{DF} phases to seek constraints on the inner core's rotation rate. Careful analysis and strict rejection criteria yield 655 PKP_{BC}–PKP_{DF} differential travel time residuals computed with respect to the AK135 reference model, densely sampling a small region of the inner core over a time period of 15 years. The data images both lateral and radial velocity heterogeneity in the inner core located geographically beneath the north Pacific between radii of 870 and 1080 km. The dominant feature is a longitudinal wave speed gradient centred at about 180° longitude. In combination with different earthquake catalogues and inner core anisotropy models, we explore different techniques to use this gradient to constrain the rotation rate. Our estimates range from 0.45 ± 0.25 to $0.74 \pm 0.29^\circ/\text{yr}$ relative to the mantle, with two of four estimates including zero rotation at the 95% (2σ) confidence level, indicating that rotation is marginally detectable. As an alternative to monotonic rotation, we find weak evidence for rotational oscillation of the inner core on time scales of about 280 days. In consequence, these observations suggest that: (1) viscous coupling between the outer and inner core simulated using viscous hyperdiffusivity is not appropriate for modelling inner core rotation; (2) temperature gradients between the interior and exterior of the tangent cylinder in the core are also small; (3) gravitational torques coupling the inner core to the mantle are large, on the order of 2×10^{21} Nm; and (4) the inner core's viscosity is high, 3.9×10^{19} Pas. © 2001 Published by Elsevier Science B.V.

Keywords: inner core rotation; PKP phases; differential travel times

1. Introduction

Since the initial seismic observations of differential rotation of the Earth's inner core relative to

the mantle [1–3] a debate has ensued regarding both the magnitude and even the existence of this rotation. Both proponents and skeptics of inner core rotation would, however, acknowledge the importance of quantifying its magnitude to enhance our understanding of the geodynamo. Prior to these initial seismic observations variable inner core rotation of around $1.8^\circ/\text{yr}$ was found by Glatzmaier and Roberts [4] in their simulation

* Corresponding author. Present address: QinetiQ, St. Andrews Road, Malvern, Worcestershire WR14 3PS, UK..

E-mail address: jonathan@gly.bris.ac.uk (J.D. Collier).

of the geodynamo. Observations of the inner core rotation rate are important since they provide constraints on properties at the inner core boundary such as viscous coupling between the inner and outer core and the toroidal magnetic field strength. Thus constraints on inner core rotation facilitate more earthlike modelling of the geodynamo.

The seismic observations [1,3,5,6] suggesting that the Earth's inner core is rotating faster than the mantle were made using measurements of the differential travel times between the core phases PKP_{DF} and PKP_{BC} (Fig. 1). These phases follow similar paths through the mantle but PKP_{DF} passes through the inner core while PKP_{BC} skims its surface. Variations in the PKP_{BC} – PKP_{DF} travel times are therefore attributed mainly to the inner core portion of the PKP_{DF} path since the outer core is essentially homogeneous. Such studies

base their conclusions on the fact that the inner core has a bulk anisotropy of 3–4% and heterogeneities in seismic velocities and that the rotation of these structures can be detected in the travel times of seismic waves which pass through it. Earthquakes in the South Atlantic recorded by stations in Alaska provided Song and Richards [1], Creager [3] and Song [6] with near-polar paths yielding estimates of $1^\circ/\text{yr}$ and 0.2 – $0.3^\circ/\text{yr}$ respectively for the rotation of the inner core faster than the mantle. More recently Song and Li [7] have used earthquakes in Alaska recorded at a South Pole station as further evidence for inner core rotation faster than the mantle by $0.6^\circ/\text{yr}$. In contrast to the relatively small number of stations used in these studies, Su et al. [2] used a global travel time data set of absolute PKP_{DF} travel times, reporting a rotation of up to $3^\circ/\text{yr}$ faster than the mantle.

Other studies of PKP_{BC} – PKP_{DF} travel time residuals come to different conclusions arguing for a small or zero differential rotation of the inner core. Souriau [8] uses nuclear tests in Novaya Zemlya recorded at a station in Antarctica to argue against any possible rotation rate greater than $1^\circ/\text{yr}$, a similar conclusion to Poupinet [9] with both a worldwide dataset and paths from Tonga to France. Meanwhile Poupinet et al. [10] used teleseismic doublets – earthquakes at similar locations and depths but separated in time – to suggest a maximum rotation rate of $0.2^\circ/\text{yr}$. Some workers (e.g. [11]) have questioned the conclusions of the PKP differential travel times studies that indicate significant rotation rates and postulated systematic hypocentre mislocation errors that influence the data without requiring rotation of the inner core. It is clear so far that body wave-based seismological estimates of inner core rotation show little consensus other than that any differential rotation is close to the resolution of the techniques used.

Inner core structure has also been investigated using splitting functions of free oscillations. Sharrock and Woodhouse [12] found evidence to support some time dependence of inner core structure using this method but suggested retrograde inner core rotation of 1 – $2^\circ/\text{yr}$ in contrast to the prograde motion found by the seismic body wave

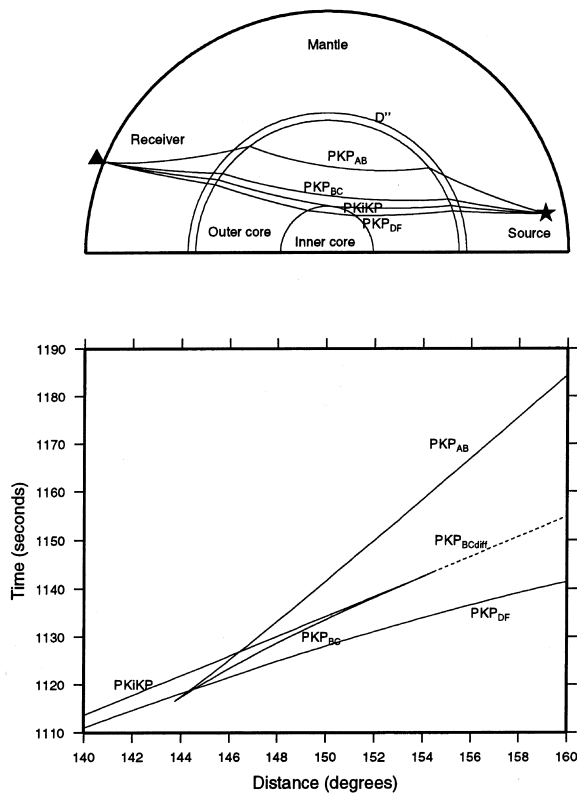


Fig. 1. (Top) Schematic showing the ray paths of the PKP phases. (Bottom) Travel time curves for the phases in the top panel from the AK135 reference model.

studies. They concluded that this time-dependent inner core structure could not therefore be attributed solely to differential rotation and postulated that some other mechanism may be required to explain the data. More recently Laske and Masters [13] in a study of the Earth's free oscillations observed $0.0 \pm 0.2^\circ/\text{yr}$ rotation, though a longer temporal database may be required to reliably constrain a slow rate of rotation [14].

In this study we are once again using body wave differential travel times to assess whether inner core rotation is observationally detectable. We investigate PKP ray paths from Tonga and Fiji earthquakes to the UK seismic network (Fig. 2). The PKP_{DF} bottoming points lie slightly south of those in a previous study by Souriau and Poupinet [9], and pass through regions of the inner core previously observed to have significant gradients in velocity [15,16], which provides an inner core marker whose change in position with time may be observed. What distinguishes this study from previous ones are two factors, both stemming from our use of a regional seismic network. Firstly, the network has been continuously operating with no sensor changes for about 25 years. Thus issues concerning instrumentation changes that may affect signal timings are eliminated. Secondly, because a single earthquake may be recorded by over 100 sensors spread over about 10° in epicentral distance, we can eliminate cycle skipping errors in the waveform picks that underlie our method. Waveform evolution may be closely monitored across the array and unusual waveforms discarded before processing. The result is a high-quality dataset in which systematic errors are reduced, lending further credibility to an assessment of inner core rotation based on it.

2. Data and method

The UK array was established in 1969 to monitor local and regional earthquakes for domestic hazard assessment purposes and is maintained by the British Geological Survey. The UK network instruments are short-period Willmore MK III instruments, and over the observational period no sensor or datalogger upgrades were made ex-

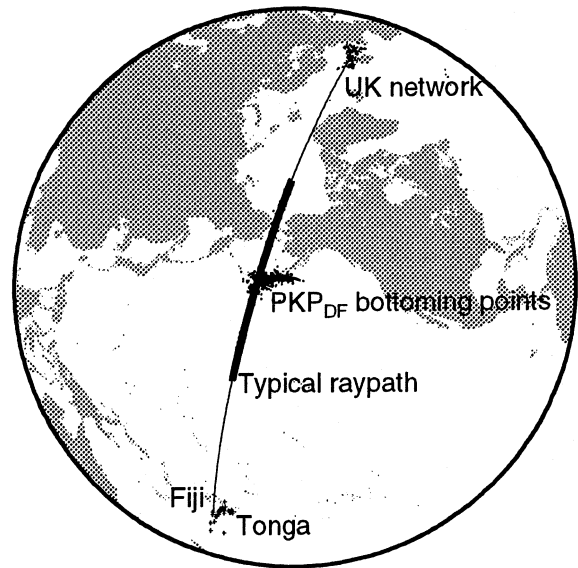


Fig. 2. Lambert azimuthal equal-area map showing source locations in Tonga/Fiji (pluses) and receiver locations in the UK (circles). A typical great circle path is shown together with the bottoming points of the PKP_{DF} rays (squares).

cept for routine servicing. Fifteen years of these data (Table 1) provides the data for this study (the recording media of earlier events we found to be irretrievably degraded). We hand-pick PKP_{DF} and PKP_{BC} arrivals for a large number of events between 1985 and 2000 (Table 1) to investigate inner core structure using PKP_{BC}–PKP_{DF} travel time residuals relative to the AK135 reference model [17]. The use of data from a dense network instead of the smaller numbers of stations used in similar studies (e.g. [1,3,7]) potentially provides a much larger quantity of data, a larger bottoming depth range of the PKP_{DF} phase and the ability to follow a waveform across the array to help avoid mis-picks. Earthquakes with magnitudes ranging from 5.0 to 6.6 m_b are used (Table 1). It is highly desirable in this kind of study to use source locations that are temporally homogeneous. Thus we use the NEIC catalogue which gives locations for all the events in the time period of our data and the EHB catalogue of relocated hypocentres [18] which covers a significant subset to the end of 1999. The NEIC catalogue shows only very small differences in source location [16] when compared to the re-

locations of Engdahl et al. [18] for Tonga and Fiji events and its use does not significantly affect the pattern of residuals seen for the pre-2000 events. We investigate the effect of using either catalogue or estimates of the inner core rotation rate later.

2.1. PKP_{BC} – PKP_{DF} residuals

Typically between 50 and 120 stations are available for each event. Tonga and Fiji earthquakes yield source/receiver distances in the range 140–160°. After discarding noisy seismograms and

Table 1
List of earthquake locations from the NEIC catalogue

Date (yyyymmdd)	Time	Latitude	Longitude	Depth (km)	Mag. (M_w)	Number of seismograms
19850427	10:11:42	–21.03	–176.82	260	5.8	14
19850828	20:50:48	–21.01	–178.98	624	6.2	24
19851012	02:12:57	–21.66	–176.38	155	6.4	4
19860526	18:40:44	–21.82	–179.08	583	6.1	12
19880115	08:40:23	–20.79	–175.99	213	6.2	4
19880310	10:25:05	–20.92	–178.65	623	6.1	2
19900528	11:28:47	–20.87	–177.99	485	5.9	12
19900626	12:08:29	–22.01	–179.47	586	6.0	26
19900722	09:26:14	–23.62	–179.89	531	5.9	44
19901010	05:54:53	–23.50	179.03	548	6.6	41
19910418	09:41:20	–22.92	–179.34	470	5.8	36
19910930	00:21:46	–20.88	–178.59	566	6.5	28
19921112	22:28:57	–22.40	–178.10	359	5.9	5
19930502	15:26:02	–21.15	–175.88	120	5.7	8
19930527	08:51:59	–29.36	–178.27	118	5.9	3
19930807	17:53:24	–23.87	179.85	523	6.7	26
19930821	09:42:35	–21.28	–178.02	426	6.1	33
19940331	22:40:52	–22.06	–179.53	579	6.5	5
19941027	22:20:28	–25.78	179.34	518	6.7	6
19961019	14:53:48	–20.41	–178.51	590	6.9	35
19961114	13:47:38	–21.24	–176.62	191	6.2	25
19970904	04:23:37	–26.57	178.34	624	6.8	56
19971008	10:47:49	–29.25	178.35	617	5.7	5
19971017	15:02:00	–20.89	–178.84	578	6.0	9
19980127	19:55:01	–22.54	179.05	611	6.3	21
19980127	21:05:44	–22.41	179.04	610	6.5	17
19980414	03:41:22	–23.82	–179.87	498	6.1	11
19980516	02:22:03	–22.23	–179.52	586	6.9	63
19980516	10:41:28	–21.79	–176.64	174	5.5	15
19981011	12:04:54	–21.04	–179.11	623	5.9	2
19981227	00:38:26	–21.63	–176.38	144	6.8	19
19990306	20:28:53	–21.73	–179.46	602	5.7	12
19990312	11:16:39	–20.00	–177.76	587	5.6	8
19990323	11:23:44	–20.91	–178.73	574	5.6	5
19990602	07:34:41	–20.86	–179.00	644	5.4	2
19990626	22:05:28	–17.96	–178.19	590	6.0	2
19990721	03:10:44	–18.29	–177.91	560	5.7	5
19991130	20:10:22	–21.33	–178.66	547	5.8	3
20000115	12:49:45	–21.22	–179.26	632	6.1	12
20000123	18:21:01	–24.90	179.56	514	5.3	6
20000318	23:22:52	–24.36	178.98	551	5.5	7
20000418	17:28:12	–20.66	–176.47	220	6.0	1
20000508	21:35:42	–31.32	179.84	383	5.7	6
20000614	02:15:25	–25.52	178.05	604	6.4	16

those for which the source to receiver distance is not in the right range ($145\text{--}155^\circ$) around 45% of the original records are usually retained. The records are low-pass filtered with a corner frequency of 2.0 Hz and manual picks are made in the PKP_{BC} and PKP_{DF} waveforms. We retain only seismograms where the PKP_{BC} and PKP_{DF} waveforms are similar and normally pick two or three pairs of peaks/troughs with the maximum being five, which leaves high-quality picks in only around 10% of the original seismograms. The uncertainty σ associated with each observation is typically $0.3 \leq \sigma \leq 0.5$ s, which is derived from the standard error of the differential times between the peak pairs picked in each seismogram.

A typical example of the short period records used is given in Fig. 3. For this event after removal of noisy records and those for which the PKP_{BC} waveform is dissimilar to those across the rest of the network 75 seismograms are left from an original 110 (Fig. 3, top). The phases PKP_{DF} , PKP_{BC} and PKP_{AB} can clearly be seen in this figure with relative arrival times very similar to those calculated from the AK135 model. The PKiKP phase cannot be observed given its close proximity to the much larger PKP_{BC} phase. Of these records only 21 are retained after a comparison of PKP_{BC} and PKP_{DF} waveforms (Fig. 3, bottom). In this example four or five pairs of picks are made in each seismogram. The mean of the PKP_{BC} – PKP_{DF} differential times and its standard deviation are then calculated. Travel time residuals were calculated from these observed differential times using the radial earth model AK135 with corrections for the Earth's ellipticity [19]. The ellipticity corrections yield variance reductions of 19.9% and 17.0% relative to the AK135 model for the EHB and NEIC locations respectively. Percentage travel time residuals were calculated by dividing these residuals by the total time that PKP_{DF} spends in the inner core [3].

3. Results

The observed travel time residuals along these paths from Tonga/Fiji to the UK are small, generally less than 1 s, and could be indicative of

heterogeneity or anisotropy anywhere along the different ray paths that PKP_{DF} and PKP_{BC} take from the source to the receiver. We consider the effects from experimental factors, the mantle, and the core in turn and then discuss the inferences that can be drawn from our observations regarding inner core rotation.

3.1. Origin in the mantle?

The global structure of the mantle has been shown in tomographic studies (e.g. [20–23]) to be heterogeneous. The PKP_{DF} and PKP_{BC} phases travel through similar paths in the mantle (Fig. 1, top) and therefore the effect of mantle heterogeneity on their travel time residuals has often been considered negligible.

In Collier and Helffrich [16] we evaluated the possible contamination of PKP_{BC} – PKP_{DF} residuals by mantle structure for paths from Tonga/Fiji to the UK by comparing our observations with the predictions of a tomographic mantle model [21]. Like Creager [24], who used a global dataset, we found that the negative correlation with the predicted values was smaller than the data scatter. We also noted that the data correlate with reported inner core velocity structure differences [25] and with the predictions of a global model of inner core heterogeneity [15], both of which were constructed without data from the ray paths that we use. Analysis of absolute arrival times showed that trends in PKP_{BC} – PKP_{DF} differential travel times correlate with trends in absolute PKP_{DF} and not PKP_{BC} times (Fig. 4a). Thus we concluded that the effects of inner core heterogeneity dominate those of the mantle which can therefore be discarded as a first order effect.

3.1.1. Origin in the core?

The core phases PKP_{DF} and PKP_{BC} are separated by the greatest distance as they pass through the Earth's core. Therefore it is reasonable to expect that core heterogeneities would have a much larger effect on their differential times than heterogeneities of similar magnitude elsewhere along their ray paths. The outer core, however, is assumed to be laterally very homogeneous [26,27], and, if radial stratification exists, we would expect

angles through the core do not vary much, the anisotropy corrections are small but must be removed to separate the influence of anisotropy from heterogeneity in the observations. In simple models, inner core anisotropy has cylindrical symmetry about an axis approximately aligned with the Earth's spin axis. We test several models of inner core anisotropy and evaluate which is most effective at removing the anisotropic signature in

the data. Most models are similar to that of Creager [32] which assumes cylindrical symmetry about the Earth's spin axis and takes the form:

$$\delta v_p (\cos^2 \xi) = A + B \cos^2 \xi + C (\cos^2 \xi)^2 \quad (1)$$

where ξ is the angle between the Earth's spin axis and the ray path through the inner core evaluated at the ray's bottoming point. In the Creager [32] model for example values for the constants are $A = 0.018$ km/s, $B = -0.165$ km/s and $C = 0.557$ km/s and the perturbations are relative to a nominal inner core $v_p = 11$ km/s. For ray paths from Tonga/Fiji to the UK typical angles between the inner core segment of the ray and the Earth's spin axis are between 46° and 58° . The various models of [24,32] yield variance increases after correction ranging from 48 to 134%, whereas the time-invariant anisotropy model of Song and Richards [1] gives a variance reduction of 24%. The corrections are largely shifts in the mean which get absorbed in the constant parameter in the fitting procedure to be described later.

3.1.3. Inner core heterogeneity

The remaining scatter in the data after correction for inner core anisotropy suggests heterogeneity in the inner core. The presence of both lateral and radial velocity gradients with respect to the AK135 model have been shown in Collier and Helffrich [16] to best explain trends in the data. These include a distinct longitudinal gradient (Fig. 4b–d) that is the feature we will use to detect rotation of the inner core with respect to the mantle.

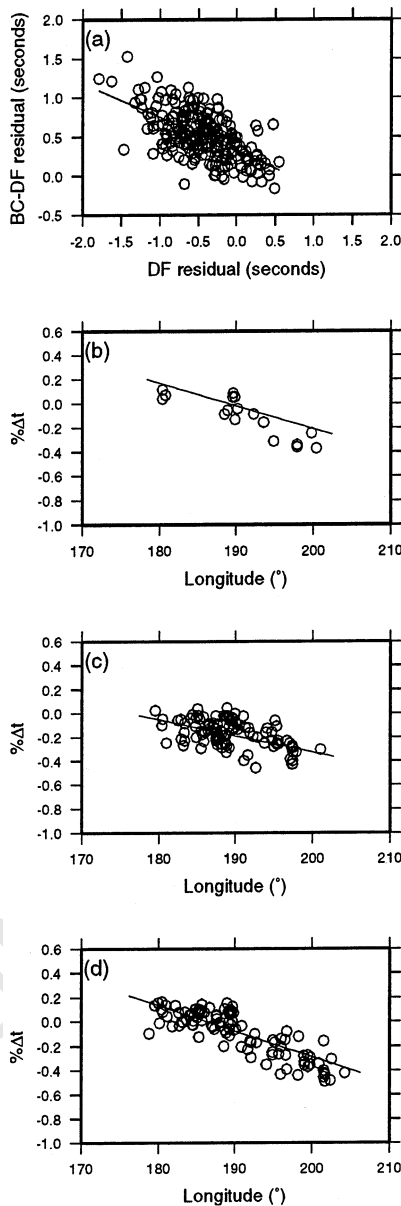


Fig. 4. Evidence that differential time signal is due to variations in inner core structure (a), and lateral gradients in the core during different epochs (b–d). (a) Early PKP_{DF} arrivals yield negative residuals (horizontal axis) that correlate with larger PKP_{BC}–PKP_{DF} differences (vertical axis). If differential time variations were due to influence of D' structure, they would yield late PKP_{DF} arrivals, and a correlation in the opposite sense (from [16]). Data shown are a subset of data used in this study for 1992–2000 where absolute times are reliable. (b–d) Longitudinal velocity gradients for data in the radius range 975–1025 km in the boxes shown in Fig. 5. Data in the time periods (b) 1985–1989, (c) 1990–1994 and (d) 1995–1999.

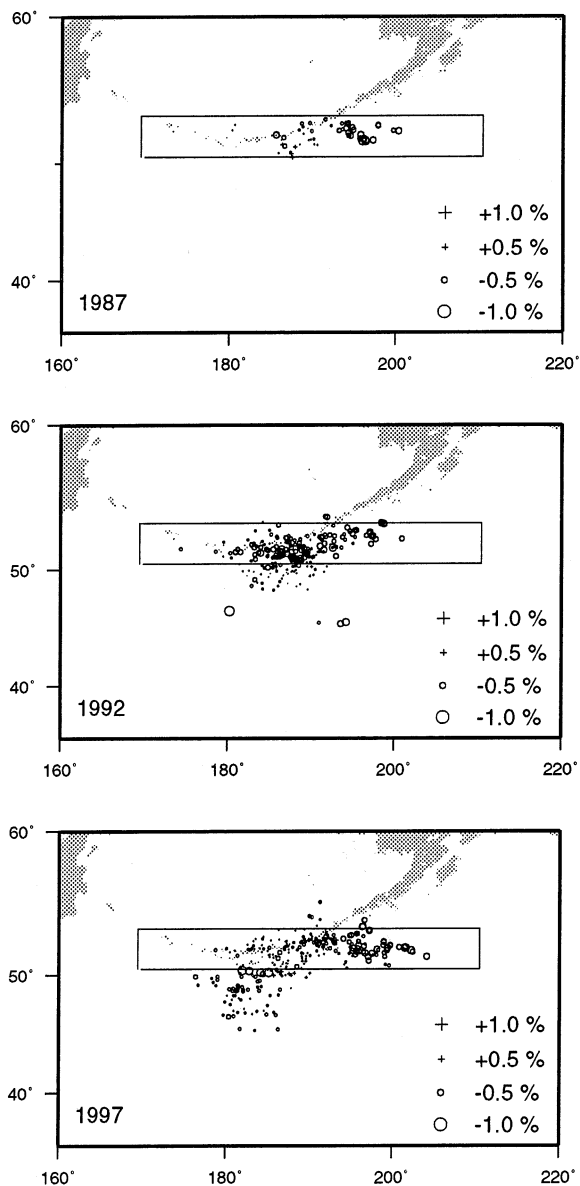


Fig. 5. Maps showing the $PKP_{BC}-PKP_{DF}$ residuals using EHB earthquake locations plotted at the PKP_{DF} bottoming point. Data in the time periods (top) 1985–1989, (middle) 1990–1994 and (bottom) 1995–1999.

3.2. Inner core rotation

The bottoming points of our data are clustered geographically beneath the north Pacific (Fig. 5), sampling a different region of the inner core to the previous inner core rotation studies of Song and

Richards [1], Su et al. [2], Creager [3], Souriau [8], Song and Li [7] and Song [6], and a little further south than Souriau and Poupinet [9]. Tanaka and Hamaguchi [15] and Collier and Helffrich [16] previously showed that a significant longitudinal velocity gradient exists in this region. In this present study, comprising 15 years of data, we seek the temporal variation in travel time residuals that would occur if this gradient was moving with respect to the sources and receivers and would thus indicate inner core rotation. We use three different techniques to attempt to detect this signal, which the subsequent sections discuss.

3.2.1. Temporal change in velocities

We can attempt to place upper bounds on an inner core solid body rotation rate by seeing whether the observed velocity gradient shifts laterally in time due to a shift in the inner core’s angular position. Fig. 4b–d shows data from a depth range of 975–1025 km from the cross-sections on the maps in Fig. 5. These cross-sections essentially isolate the longitudinal velocity gradients from the radial and latitudinal ones. Since the trend with longitude is well-described by a straight line, we fit lines to each set of fractional travel time differences. Table 2 lists the parameter estimates.

A reconnaissance of the data shown in Fig. 4 immediately rules out large rotation rates. The longitudinal data spread around the line is about $\pm 10^\circ$. If there were rotations as large as $3^\circ/\text{yr}$, the trend in the epoch centred on 1987 would be visibly shifted 30° eastward in longitude, yet the epoch 1997 data do not show this. Monotonic rotation rates larger than about $1^\circ/\text{yr}$ are unlikely given the trends and dispersion in the observed differential time anomalies. We thus anticipate

Table 2

Fit information for the data in Fig. 4 to a model of the form $y = a + b\lambda$

Epoch	N	χ^2	a (s)	b (s°)
1987	22	1.3	6.056 ± 1.094	-0.03282 ± 0.00575
1992	123	12.2	4.346 ± 0.459	-0.02373 ± 0.00243
1997	91	14.0	2.910 ± 0.478	-0.01530 ± 0.00256

that any rotation derived from the data will be small.

One way to test for rotation is to assume a constant longitudinal gradient in the core whose zero crossing shifts with time due to inner core rotation. The weighted average longitudinal gradient of all the data is $-2.078 \times 10^{-2} \text{ s}^\circ$, which is within the 99% confidence level of the derived gradient in each epoch. Fitting each epoch's data in turn with this gradient, we obtain zero crossings at $190.4 \pm 1.4^\circ$ (1987), $183.2 \pm 0.5^\circ$ (1992), and $190.2 \pm 0.8^\circ$ (1997). The crossings do not show a longitudinal progression through time, nor does the longest span (1987–1997) show a significant difference in zero crossings. The 1987–1992 epoch difference suggests a westward rotation rate of $1.42 \pm 0.38^\circ/\text{yr}$, and the 1992–1997 difference suggests an eastward rotation rate of $1.40 \pm 0.26^\circ/\text{yr}$. This analysis scheme therefore suggests no monotonic inner core rotation. Oscillatory inner core motion is possible, as some numerical models of dynamo action suggest [36,37]. We defer the analysis for oscillatory core behaviour to a later section.

3.2.2. Summary rays

Souriau and Poupinet [9] observed that PKP_{DF} summary rays, calculated from those rays with a similar geometry in the inner core, were always calculated without taking into account inner core rotation. They investigated possible inner core rotation by searching for a minimum in the standard deviations of the mean of the travel time residuals in different cells in the inner core. In this study we have a shorter time span, but this is countered by the very high density of our data which ameliorates the trade-off between cell size and the number of rays per cell. We calculate summary rays for cells in the inner core with approximately equal lengths to each of their sides. Experimentation leads us to the conclusion that the optimum cell size for our data lies between 25 and 100 km. Fig. 6 shows results for a cell size of 75 km with a minimum of 30 rays in each cell. The minimum of the mean standard deviation is shown to occur for a rotation rate near 0.0°/yr relative to the mantle for our data. However, as in the study of Souriau and Poupinet [9], our

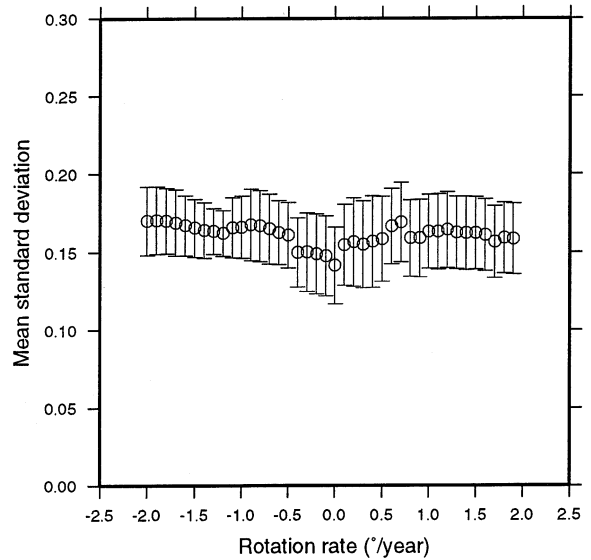


Fig. 6. Mean standard deviations for PKP_{BC}–PKP_{DF} summary ray residuals. The cells in which the summary rays are calculated have sides of length 75 km. The minimum mean standard deviation indicates a zero rotation rate. The error bars represent the standard deviation of the mean.

error bars are large making this an imprecise method.

3.2.3. Linear modelling

An alternative method for measuring the inner core rotation rate is to model the three-dimensional variation of wave speeds in the inner core, similar to the approaches taken by Creager [3], Song and Li [7] and Song [6], but here with an additional term dependent on the latitude. The fractional velocity anomaly $\varepsilon = \delta v/v$ averaged along the inner core ray path and assigned to the PKP_{DF} bottoming point is assumed to depend on the longitude (λ), the latitude (θ), the inner core rotation rate (α), the bottoming depth (d) and the time (T) via:

$$\varepsilon(\lambda, d, T) = \varepsilon_0 + \frac{\partial \varepsilon}{\partial \lambda}(\lambda - \lambda_0) + \frac{\partial \varepsilon}{\partial \theta}(\theta - \theta_0) + \frac{\partial \varepsilon}{\partial d}(d - d_0) - \frac{\partial \varepsilon}{\partial \lambda} \alpha (T - T_0) \quad (2)$$

T_0 , λ_0 , d_0 and θ_0 are the reference time, longitude, depth and latitude. We assume that the inner core spin axis coincides with the Earth's, in accord

with the removal of the effect of inner core anisotropy. A west to east rotation of the inner core would result in a positive value for α . In order to separate the combined $\alpha \times \partial \epsilon / \partial \lambda$ from the $\partial \epsilon / \partial \lambda$ dependence and minimise the uncertainty in α , we first minimise χ^2 by varying α and fitting the first four terms of Eq. 2 to the data shifted in longitude by $-\alpha(T-T_0)$. This method yields an uncertainty for α by $\Delta\chi^2$, and for the remaining parameters by their least-squares errors [38], shown in Fig. 7. We invert the data in the region with the largest time span of data, shown by the boxes in Fig. 5. Table 3 summarises our results for different model fits using the locations from the NEIC and EHB catalogues and correcting for inner core anisotropy using a suite of models. Variance reductions of 59–84% result from the fits. The reductions appear to depend on the particular anisotropy corrections applied, but are similar for different catalogues. This suggests that 10–15% of the data variance lies in the catalogue used to reduce the travel times. The remainder is due to inner core structure.

Our estimates of the inner core rotation rate by this method are between 0.45 and 0.74°/yr pro-

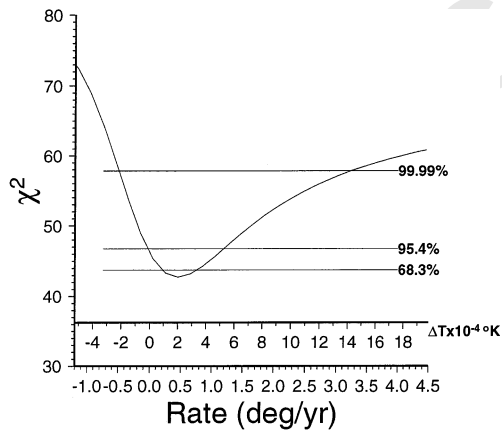


Fig. 7. χ^2 minimisation as a function of the assumed rotation rate (lower axis) for method d in Table 3. The confidence levels associated with the rotation rate of 0.45°/yr are $\pm 0.25^\circ/\text{yr}$ (68.3% conf.), through $\pm 1.85^\circ/\text{yr}$ (99.99% conf.). Upper axis is rotation rate converted into the temperature difference ΔT between interior and exterior of inner core tangent cylinder in a simplified core model [42]. At the 99.99% confidence level, ΔT could be as low as -0.2 mK or as high as $+1.4$ mK, but due to the model's simplicity, should only be viewed as suggestive.

Table 3
Results from the modelling of the data in the boxes in Fig. 5

Model	Loc. ^{a)}	N_{obs}	Ani. corr. ^{b)}	ϵ_0	$\partial \epsilon / \partial \lambda$ (1/°)	$\partial \epsilon / \partial \theta$ (1/°)	$\partial \epsilon / \partial d$ (1/km)	α (°/yr)	% Var. red.
a	NEIC (386)	C92		$2.862 \times 10^{-3} \pm 2.572 \times 10^{-4}$	$1.420 \times 10^{-4} \pm 2.448 \times 10^{-5}$	$2.066 \times 10^{-4} \pm 2.222 \times 10^{-4}$	$3.233 \times 10^{-5} \pm 7.543 \times 10^{-6}$	0.74 ± 0.29	82
b	NEIC (386)	SR96		$1.215 \times 10^{-3} \pm 2.566 \times 10^{-4}$	$1.642 \times 10^{-4} \pm 2.558 \times 10^{-5}$	$6.390 \times 10^{-4} \pm 2.223 \times 10^{-4}$	$3.303 \times 10^{-5} \pm 7.547 \times 10^{-6}$	0.64 ± 0.25	63
c	EHB (376)	C92		$2.947 \times 10^{-3} \pm 2.601 \times 10^{-4}$	$1.453 \times 10^{-4} \pm 2.721 \times 10^{-5}$	$2.759 \times 10^{-4} \pm 2.216 \times 10^{-4}$	$3.164 \times 10^{-5} \pm 8.016 \times 10^{-6}$	0.53 ± 0.28	83
d	EHB (376)	SR96		$1.308 \times 10^{-3} \pm 2.597 \times 10^{-4}$	$1.577 \times 10^{-4} \pm 2.801 \times 10^{-5}$	$7.131 \times 10^{-4} \pm 2.216 \times 10^{-4}$	$3.236 \times 10^{-5} \pm 8.019 \times 10^{-6}$	0.45 ± 0.25	61

Model reference values (λ_0 , θ_0 , T_0) are (52.75°N, 170.00°W, 215 km, 1992.0 yr).

^{a)} Hypocentral catalogue: EHB: Engdahl et al. [18]; NEIC: National Earthquake Information Center.

^{b)} C92: Creager [32]; SR96: Song and Richards [1]. C92 listed because it yields largest α ; other models from Creager [24] yield $0.47 \leq \alpha \leq 0.74^\circ/\text{yr}$ and $0.25 \leq \sigma_\alpha \leq 0.29^\circ/\text{yr}$.

grade relative to the mantle. At the 95% confidence level (2σ) the rotation rate is indistinguishable from zero for residuals against locations for the EHB catalogue (c and d) and at the 99% (3σ) confidence for all of the tabulated models.

3.2.4. Oscillatory modelling

The inner core may oscillate around a fixed position relative to the mantle at periods between about 1 and 10 years [37], which our dataset, with its 15-year span, is capable of detecting. We seek this by computing the spectral power of the differential travel time anomalies with a method capable of dealing with irregularly spaced data [38]. To de-emphasise the dominance in the overall fit of events with more seismograms, we reduce each event to a single summary residual characterised by the median δt , λ , and σ , yielding 33 events in the 15-year data interval. To reduce the signal to perturbations around a constant value, we remove the trend in the residuals by subtracting the best-fit longitudinal gradient (see Section 3.2.3, -2.078×10^{-2} s/°). In all combinations of processing methods (Table 3), the largest spectral peak is at a frequency of 1.3/yr (280 days), but its significance varies. In the best case, the peak is significant at the 97% confidence level in combination a (see Table 3) and accounts for 50% of the variance of the data. This is illustrated in Fig. 8. This best-fitting sinusoid has an amplitude of $1.94 \pm 1.03 \times 10^{-1}$ s and a phase of -47° relative to 1992.0, and implies oscillations of $9.3 \pm 9.3^\circ$ around a stationary position, which is compatible with the epoch-based analysis reported earlier. Confidence levels for the remaining processing methods b–d are 93%, 96%, and 89% respectively. The earthquake locations, anisotropy correction models used, and lateral gradients adopted affect the significance of the spectral peak, but not its position. Random, synthetic residuals using the same earthquake dates and bottoming positions and processed similarly yield no spectral peaks above the 55% confidence level. Thus there is evidence suggesting oscillatory motion of the inner core in our dataset, but it is not overwhelmingly convincing.

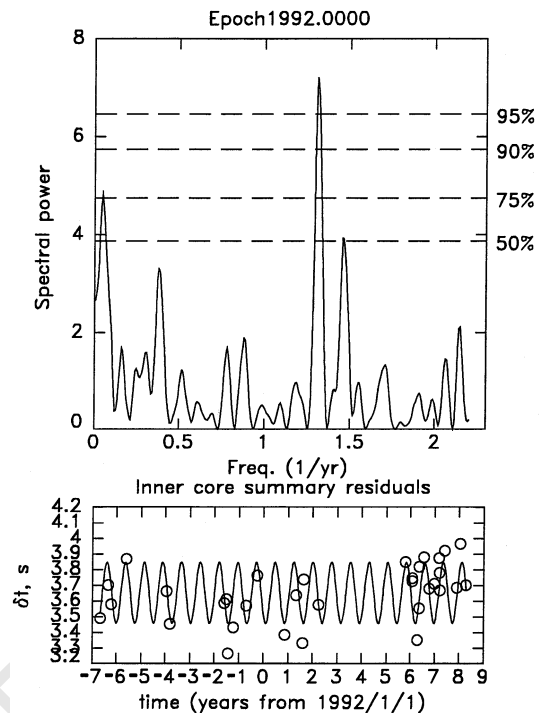


Fig. 8. Test for oscillatory component in travel time residuals. Spectrum of travel time residuals for processing method a in Table 3 (top) and best-fitting sinusoid corresponding to the spectral peak at 1.3/yr (bottom). Dashed lines on the spectrum correspond to confidence levels that the peak is not a random occurrence, showing that only one peak is significant. The sinusoid explains 50% of the variance in the summary residuals.

4. Discussion

In this effort to detect inner core rotation, we used a known longitudinal gradient in the velocity structure as a marker and sought the secular change in travel times that it would cause if the inner core were rotating. We used a regional array to obtain differential $PKP_{BC}-PKP_{DF}$ travel times, which ameliorated problems with identifying corresponding parts of the PKP waveforms by following waveform features as they evolved across adjacent portions of the array, leading to high-quality travel time picks. Throughout the 15-year period of our study, the underlying seismic instrumentation did not change, eliminating one potential error source of secular changes in observed travel times. Our estimates of the mono-

tonic inner core rotation rate are $0.45\text{--}0.74^\circ/\text{yr}$ and might reasonably be interpreted as zero. Like virtually all other estimates however, they suggest that the inner core is rotating marginally faster than the mantle. Our results are compatible with some of the previous values that are close to zero: the body wave studies of Creager [3], Song and Li [7], the free oscillation studies of Laske and Masters [13] and Masters [39] and the inner core scattering study of Vidale et al. [40]. We can conclude from the convergence between our results and those from these other studies that the inner core rotation rate is probably closer to zero than the larger values suggested by some other body wave studies [1,2,6]. Our observations (Fig. 4) clearly rule out rotation rates in excess of $\pm 3^\circ/\text{yr}$, and $\pm 1^\circ/\text{yr}$ at the 95% confidence level.

One curious feature to emerge in the analysis is that there is some evidence for the oscillation of the inner core. Split into 5-year epochs, there is a change between the gradient's inferred position that suggests westward movement in the epochs centred in 1987–1992, and then eastward movement between the epochs centred on 1992 and 1997. This long-term oscillation may be aliasing of a shorter-term oscillation suggested by a spectral analysis of the travel time residuals. The residual spectrum contains significant power at oscillation frequencies corresponding to about 280 days. This spectral peak maintains its position despite changing the catalogue, the anisotropy model used to reduce the observed differential times to residuals, or the longitudinal gradient adopted within the range allowed by the data. However, the significance of the peak degrades to levels that would falsely report a spectral peak in random data as much as 11% of the time. Whether this feature is real or not will await a future study using denser sampling in time of this section of the inner core.

The inferred inner core rotation rate is related to the physical state of the inner core and the way it interacts with the core and mantle mechanically, electromagnetically and gravitationally. One immediate consequence of a small-to-zero rotation rate is that it excludes the class of dynamo simulations using viscous hyperdiffusivity with viscous coupling to the inner core. A significant difference

between Glatzmaier and Roberts [4] simulation, in which the inner core rotates monotonically at rates of $1.8^\circ/\text{yr}$ or more, and other simulations lacking viscous coupling or hyperdiffusivity [36,41] are slow or oscillating inner core rotation rates, that we find here. Another feature of the core that rotation bears upon is the magnitude of the thermal winds that operate inside the inner core's tangent cylinder in the outer core. Aurnou et al. [42] find that extremely small temperature gradients in the outer core can drive rotation of the inner core by developing a thermal wind in the tangent cylinder that drags the poloidal magnetic field lines that thread the inner core and drives its rotation relative to the mantle. In the framework of this model, the temperature difference between the interior and exterior of the tangent cylinder is linearly related to the rotation rate, but it could also be due to differential light-element release rates. Fig. 7 shows the scaling between inferred rotation rate and the temperature difference, using standard parameter values [42]. These small, milli-Kelvin level differences inside and outside the tangent cylinder should only be viewed as suggestive due to the simplicity of the model in its neglect of gravitational torques and electrical torque balance outside the tangent cylinder itself.

Whether the observations support oscillation of the inner core is speculative on account of the variable statistical significance of the spectral peak (Fig. 8). Despite the uncertain significance, the frequency of this peak does not change with data reduction method, and stands at $1.3/\text{yr}$ or 280 days. Electromagnetic, gravitational and mechanical torques all act upon the inner core to move it relative to the mantle. An analysis of the relative magnitudes of these contributions indicates that the electromagnetic and gravitational torques are the greatest and of roughly equal magnitude, and mechanical torques are about 3–6 orders of magnitude lower [37]. Electromagnetic torque dominance leads to monotonic angular displacement of the inner core with time. In contrast, gravitational torque dominance leads to angular oscillations in the inner core's position, whose period depends on the torque strength. Roughly equal magnitudes generate combinations of these states: either progressive or jerky mono-

tonic rotation with a short-period component superimposed due to gravitational restoring torques.

Frequencies as high as 1.3/yr suggest gravitational torques F_g on the order of 2×10^{21} Nm. This is at the high end of the anticipated range, and, coupled with a low mean inner core rotation rate, suggests correspondingly weaker electromagnetic torques and a system dominated by gravitational coupling to the mantle. The attenuation of these oscillations over time yields a further constraint on the viscosity of the core, through the relationship between Q and viscosity. We can estimate the attenuation from the line width in the power spectrum [43] through:

$$Q^{-1} = \frac{\Delta f}{f_0} \quad (3)$$

where Δf is the line width at half-maximum and f_0 is the peak position: Q is about 63. Treating the inner core as a Maxwell solid [43], whose Q is:

$$Q = 2\pi f \eta / \mu \quad (4)$$

for a core rigidity μ of 160 GPa [44], we estimate the viscosity to be 3.9×10^{19} Pas. This range is in the high viscosity regime identified by Buffett [45] previously but considered unlikely because it appears to be incompatible with long-term monotonic rotation rates. If this viscosity estimate is correct, mechanical consistency forces one to infer a zero mean rotation rate from the seismological observations if the oscillation of the inner core is real and the gravitational torque is large [41]. It leads, however, to a consistent view of a non-deforming inner core as essentially locked to the mantle, but slowly oscillating rotationally with respect to it. We caution that while our data suggest that an oscillatory signal is present, more work is warranted to establish its reality more firmly.

5. Conclusions

The use of the UK seismic network has allowed us to achieve a high sampling density of data in a

region of the inner core beneath the north Pacific. Our data shows heterogeneity at radii between 870 and 1080 km in the inner core, and, most significantly, a gradient in inner core wavespeeds with longitude. Using this as a marker in the inner core, we can assess the possibility that the inner core rotates by seeking a temporal change in the gradient.

A weak temporal dependence of the travel time residuals is suggested by the data. Our best estimate for the rotation rate lies between $0.42 \pm 0.22^\circ/\text{yr}$ and $0.66 \pm 0.24^\circ/\text{yr}$ faster than the mantle for the four combinations of catalogues and anisotropy models used, and is non-zero at the 95% confidence level for two of the models reduced with the same earthquake location catalogue. The observations rule out rotation rates in excess of about $3^\circ/\text{yr}$, and rates larger than $1^\circ/\text{yr}$ are highly improbable. Additionally, we find permissive evidence for an oscillatory component to the inner core's rotation with a period of 280 days. These low-to-zero estimates of the rotation rate suggest that viscous effects may be neglected in the mechanical aspects of dynamo modelling of the core (though they still may play an important electromagnetic role), and that temperature differences (or equivalently the light-element release rates) between the interior and the exterior of the tangent cylinder are small. On the other hand, the short periodicity of the oscillatory component suggests large gravitational torques coupling the inner core to the mantle, whose size exceeds the electromagnetic ones.

Acknowledgements

We thank the British Geological Survey and their staff for access to archived and AutoDRM UK network data. J.C. thanks Annie Souriau for providing travel time residual data and Bob Engdahl for supplying earthquake relocations. We thank Satoshi Kaneshima and Masaki Matsushima for comments and our two anonymous reviewers for timely and helpful reviews, but accept blame for any remaining mistakes, oversights or omissions. Some figures were created with GMT

software [46,47]. J.C. was funded by a NERC PDRA during this work. [SK]

References

- [1] X. Song, P.G. Richards, Seismological evidence for differential rotation of the Earth's inner core, *Nature* 382 (1996) 221–224.
- [2] W.-J. Su, A.M. Dziewonski, R. Jeanloz, Planet within a planet: Rotation of the inner core of Earth, *Science* 274 (1996) 1883–1887.
- [3] K.C. Creager, Inner core rotation rate from small-scale heterogeneity and time-varying travel times, *Science* 278 (1997) 1284–1288.
- [4] G.A. Glatzmaier, P.H. Roberts, A three-dimensional self-consistent computer simulation of a geomagnetic field reversal, *Nature* 377 (1995) 203–209.
- [5] W.-J. Su, A.M. Dziewonski, Inner core anisotropy in three dimensions, *J. Geophys. Res.* 100 (1995) 9831–9852.
- [6] X. Song, Joint inversion for inner core rotation, inner core anisotropy, and mantle heterogeneity, *J. Geophys. Res.* 105 (2000) 7931–7943.
- [7] X. Song, A. Li, Support for differential inner core super-rotation from earthquakes in Alaska recorded at South Pole station, *J. Geophys. Res.* 105 (2000) 623–630.
- [8] A. Souriau, New seismological constraints on differential rotation of the inner core from Novaya Zemlya events recorded at DRV, Antarctica, *Geophys. J. Int.* 134 (1998) F1–F5.
- [9] A. Souriau, G. Poupinet, Inner core rotation: a test at the worldwide scale, *Phys. Earth Planet. Inter.* 118 (2000) 13–27.
- [10] G. Poupinet, A. Souriau, O. Coutant, The existence of an inner core super-rotation questioned by teleseismic doublets, *Phys. Earth Planet. Inter.* 118 (2000) 77–88.
- [11] A. Souriau, P. Roudil, B. Moynot, Inner core differential rotation: Facts and artefacts, *Geophys. Res. Lett.* 24 (1997) 2103–2106.
- [12] D.S. Sharrock, J.H. Woodhouse, Investigation of time dependent inner core structure by the analysis of free oscillation spectra, *Earth Planets Space* 50 (1998) 1013–1018.
- [13] G. Laske, G. Masters, Limits on differential rotation of the inner core from an analysis of the Earth's free oscillations, *Nature* 402 (1999) 66–69.
- [14] F.A. Dahlen, Latest spin on the core, *Nature* 402 (1999) 26–27.
- [15] S. Tanaka, H. Hamaguchi, Degree one heterogeneity and hemispherical variation of anisotropy in the inner core from PKP_{BC}-PKP_{DF} times, *J. Geophys. Res.* 102 (1997) 2925–2938.
- [16] J.D. Collier, G.R. Helffrich, Heterogeneity in the inner core, not the mantle, responsible for trends in PKP_{BC}-PKP_{DF} residuals in United Kingdom network data, *Phys. Earth Planet. Inter.* (2001) submitted.
- [17] B.L.N. Kennett, E.R. Engdahl, R. Buland, Constraints on seismic velocities in the earth from traveltimes, *Geophys. J. Int.* 122 (1995) 108–124.
- [18] E.R. Engdahl, R. van der Hilst, R. Buland, Global teleseismic earthquake relocation with improved travel times and procedures for depth determinations, *Bull. Seis. Soc. Am.* 88 (1998) 722–743.
- [19] A.M. Dziewonski, F. Gilbert, The effect of small, aspherical perturbations on travel times and re-examination of the corrections for ellipticity, *Geophys. J. R. Astron. Soc.* 44 (1976) 7–17.
- [20] S.P. Grand, Mantle shear structure beneath the Americas and surrounding oceans, *J. Geophys. Res.* 99 (1994) 11591–11621.
- [21] S.P. Grand, R.D. van der Hilst, S. Widiyantoro, Global seismic tomography: A snapshot of convection in the earth, *GSA Today* 7 (1997) 1–7.
- [22] B.L.N. Kennett, S. Widiyantoro, R.D. van der Hilst, Joint seismic tomography for bulk sound and shear wave speed in the Earth's mantle, *J. Geophys. Res.* 103 (1998) 12469–12493.
- [23] H. Bijwaard, W. Spakman, E.R. Engdahl, Closing the gap between regional and global travel time tomography, *J. Geophys. Res.* 103 (1998) 30055–30078.
- [24] K.C. Creager, Large-scale variations in inner core anisotropy, *J. Geophys. Res.* 104 (1999) 23127–23139.
- [25] S. Kaneshima, Mapping heterogeneity of the uppermost inner core using two pairs of core phases, *Geophys. Res. Lett.* 23 (1996) 3075–3078.
- [26] A. Morelli, A.M. Dziewonski, Topography of the core-mantle boundary and lateral homogeneity of the liquid core, *Nature* 325 (1987) 678–683.
- [27] B.A. Buffett, Earth's core and the geodynamo, *Science* 288 (2000) 2007–2012.
- [28] A. Morelli, A.M. Dziewonski, J.H. Woodhouse, Anisotropy of the inner core inferred from PKIKP travel-times, *Geophys. Res. Lett.* 13 (1986) 1545–15483.
- [29] J.H. Woodhouse, D. Giardini, X.D. Li, Evidence for inner core anisotropy from free oscillations, *Geophys. Res. Lett.* 13 (1996) 1549–1552.
- [30] L. Vinnik, B. Romanowicz, L. Breger, Anisotropy in the center of the inner core, *Geophys. Res. Lett.* 21 (1994) 1671–1674.
- [31] X. Song, Anisotropy of the Earth's inner core, *Rev. Geophys.* 35 (1997) 297–313.
- [32] K.C. Creager, Anisotropy of the inner core from differential travel times of the phases PKP and PKIKP, *Nature* 356 (1992) 309–314.
- [33] P.M. Shearer, Constraints on inner core anisotropy from ISC PKP_{DF} data, *J. Geophys. Res.* 99 (1994) 19647–19659.
- [34] X. Song, D.V. Helmberger, Anisotropy of Earth's inner core, *Geophys. Res. Lett.* 20 (1993) 2591–2594.
- [35] X. Song, D.V. Helmberger, Depth dependence of anisotropy of Earth's inner core, *J. Geophys. Res.* 100 (1995) 9805–9816.

- [36] W. Kuang, J. Bloxham, An earth-like numerical dynamo model, *Nature* 389 (1997) 371–374.
- [37] J. Aurnou, P. Olson, Control of inner core rotation by electromagnetic, gravitational and mechanical torques, *Phys. Earth Planet. Inter.* 117 (2000) 111–121.
- [38] W.H. Press, B.P. Flannery, S.A. Teukolsky, W.T. Vetterling, *Numerical Recipes in Fortran*, Cambridge University Press, Cambridge.
- [39] G. Masters, G. Laske, F. Gilbert, Autoregressive estimation of the splitting matrix of free-oscillation multiplets, *Geophys. J. Int.* 141 (2000) 25–42.
- [40] J.E. Vidale, D.A. Dodge, P.S. Earle, Slow differential rotation of the earth's inner core indicated by temporal changes in scattering, *Nature* 405 (2000) 445–448.
- [41] B.A. Buffett, G.A. Glatzmaier, Gravitational braking of inner-core rotation in geodynamo simulations, *Geophys. Res. Lett.* 27 (2000) 3125–3128.
- [42] J. Aurnou, D. Brito, P. Olson, Mechanics of inner core super-rotation, *Geophys. Res. Lett.* 23 (1996) 3401–3404.
- [43] A. Ben-Menahem, S.J. Singh, *Seismic Waves and Sources*, Dover Publications, Mineola, NY.
- [44] A.M. Dziewonski, D.L. Anderson, Preliminary reference earth model, *Phys. Earth Planet. Inter.* 25 (1981) 297–356.
- [45] B.A. Buffett, Geodynamic estimates of the viscosity of the Earth's inner core, *Nature* 388 (1997) 571–573.
- [46] P. Wessel, W.H.F. Smith, Free software helps map and display data, *EOS* 72 (1991) 441, 445–446.
- [47] P. Wessel, W.H.F. Smith, New improved version of Generic Mapping Tools released, *EOS* 76 (1998) 579.

UNCORRECTED PROOF